# Journal of Materials Chemistry A



PAPER

View Article Online

View Journal | View Issue



Cite this: *J. Mater. Chem. A*, 2017, 5, 21505

transesterification reaction<sup>†</sup>
Lu Lu, □ ‡ Jian Pan‡§ and Guogiang Li □ \*

Recyclable high-performance epoxy based on

Received 21st July 2017 Accepted 19th September 2017

DOI: 10.1039/c7ta06397k

rsc li/materials-a

Self-healing thermoset epoxy based on dynamic covalent bond chemistry has been developed in the past several years, which warrants the creation of recyclable epoxy. However, the existing systems produce epoxy that has lower strength, stiffness, and glass transition temperature, making them unsuitable for load-bearing structures. In this study, we developed a new recyclable thermoset epoxy through solid form recycling. The epoxy has strength, stiffness, and glass transition temperature similar to those found in conventional thermoset epoxy. The effect of healing temperature, healing time, healing pressure, and powder size on the healing efficiency was experimentally investigated. It was found that the healing efficiency is as high as 88.1%, and the epoxy can be recycled more than one time.

# 1. Introduction

Epoxy thermosets are typically fabricated for high strength composites or coatings because of their high crosslink density, low shrinkage, high rigidity, low creep, and good wettability as well as chemical inertness and solvent resistance. However, once small cracks are generated in the epoxy matrix, the damage will easily propagate due to the brittleness of the thermoset network. Sometimes, the damage is invisible to the naked eye and inaccessible such as in the case of laminated composites under transverse low velocity impact. Herefore, lightweight composite structures will greatly benefit if the self-healing ability of epoxy thermosets can be enabled.

Incorporating a microencapsulated healing agent and catalyst within the epoxy is the most common method for constructing self-healing thermosets. <sup>5-19</sup> Such a self-healing process is triggered by releasing the healing agent into the crack volume once the material is damaged. Another strategy is to disperse the thermoplastic healing agent into the epoxy matrix, <sup>20,21</sup> which is more effective with a shape memory epoxy matrix to heal wide-open cracks. <sup>22,23</sup> A recent development in self-healing thermoset epoxy was realized *via* introducing dynamic chemical bonds within the epoxy network. The dynamic chemical bond formation at the crack interface enables self-healing of the epoxy matrix. <sup>24-26</sup> For example, an epoxy network that can rearrange its topology by exchange reactions without depolymerization was designed based on transesterification. <sup>24</sup> Later,

Department of Mechanical & Industrial Engineering, Louisiana State University, Baton Rouge, LA 70803, USA. E-mail: lguoqi1@lsu.edu; Tel: +1-225-578-5302

§ Visiting Ph.D. student from the School of Mechanical Engineering, Nanjing University of Science and Technology, Xiaolingwei 200, Nanjing 210094, China. the transesterification reaction was used with or without catalyst for self-healing and -assembling thermoset epoxies and was systematically studied and compared.<sup>25,27</sup> Other self-healing epoxy systems based on dynamic chemical bonds include reversible Diels-Alder reaction,<sup>1,28,29</sup> reversible C-ON bond scission in alkoxyamine,<sup>30</sup> and thermally activated ester exchange.<sup>31</sup> The self-healing of epoxy coatings can also be achieved in a similar manner by embedding microcapsules,<sup>32-34</sup> nano-containers,<sup>35,36</sup> or introducing dynamic chemical bonds into the epoxy matrix.<sup>37</sup>

Fiber-reinforced polymer composites are among the materials with the highest strength-to-weight ratio and are commonly used as lightweight high-performance structural materials. Carbon fiber-reinforced epoxy resin composites have been widely used in transportation vehicles, wind turbine blades, the electronic industry, and sports/entertainment products.38 Because the cured epoxy resin is insoluble and infusible, recycling of epoxy resin is a challenge. With the increased use of thermoset epoxy in various industries, recycling has become an urgent issue. Previously developed recycling methods include mechanical, thermal, and chemical strategies. 38,39 However, most recycling methods are developed to recover carbon fiber. For those that can recycle both fiber and matrix, such as dissolution with a small-molecule solvent, the epoxy matrix with dynamic covalent bonds has low strength (tensile strength approximately 2 MPa), low stiffness (modulus approximately 3 MPa), and low glass transition temperature (approximately 33 °C), which limit its application in loadcarrying structures.40 Considering the large amount of epoxy consumed annually in load-bearing structures, it will be of great economic and environmental significance to develop a new epoxy network that has high strength, high stiffness, and high glass transition temperature, and at the same time, can be recycled and reused.

 $<sup>\</sup>dagger$  Electronic supplementary information (ESI) available. See DOI: 10.1039/c7ta06397k

<sup>†</sup> Co-first author.

The self-healing capability of thermoset epoxy with dynamic covalent bonds warrants recycling. Several recyclable thermoset epoxies based on dynamic covalent bonds have been developed in the form of powders.24,41,42 However, they again are flexible networks and not suitable for load-bearing structures. We previously developed a new self-healing epoxy with shape memory effect to facilitate crack closure.43 With shape memory effect, minimal external aid is required during the healing event. However, there are still limitations associated with the developed system, which include: (1) the compressive and tensile strengths of the as-prepared epoxy are relatively low at both room and elevated temperatures as compared to conventional epoxy systems, which still limits their use as structural materials; (2) the healing process is relatively slow (up to 52 hours); and (3) the healing efficiency is comparatively low (maximum 59%). Therefore, there is clearly a need to develop a system that produces epoxy with enhanced mechanical, thermal, and self-healing properties. Herein, we report a new system that produces epoxy featuring higher glass transition temperature, greater mechanical strength, faster healing speed, and higher healing efficiency.

# 2. Materials and methods

#### 2.1 Synthesis of recyclable epoxy

Diglycidyl ether of bisphenol A (DGEBA), phthalic anhydride, and zinc acetylacetonate hydrate powder were purchased from Sigma-Aldrich (St. Louis, MO, USA) and used without further purification. To prepare the recyclable epoxy, first, 7.74 g (0.0294 mol) catalyst zinc acetylacetonate hydrate was dissolved in 200 g (0.586 mol) DGEBA at 150 °C. Then, 43.5 g (0.294 mol) phthalic anhydride was added to the mixture. Continuous stirring was necessary to accelerate dissolution before curing occurred. The molar ratio of DGEBA to anhydride is  $2:1.^{24}$  After dissolution of the components, the mixture was poured into a PTFE mold and allowed to cure at 130 °C for 6 h.<sup>44</sup> The oven was then turned off, and the sample was allowed to cool slowly overnight. A transparent brown solid was obtained (Fig. 1a). A flowchart of the sample preparation process is included in Fig. S1 in the ESI.†

#### 2.2 Recyclable epoxy powder preparation

The as-prepared epoxy was first cut into strips using a saw cutting machine. Then, the material was hammered into

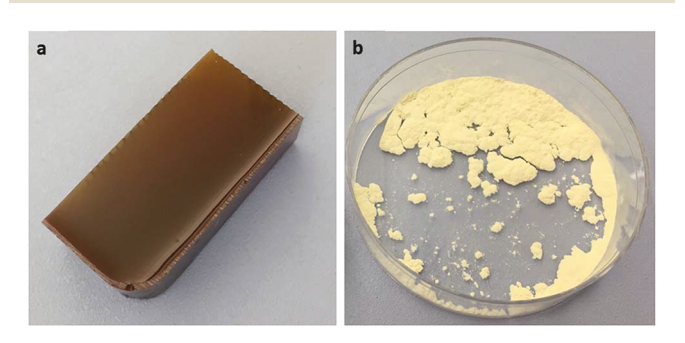


Fig. 1 Photographs of (a) the as-prepared epoxy and (b) the epoxy powder after 8 h of ball milling.

smaller pieces. These pieces were separated into two portions of similar weight and placed into the alumina ceramic grinding jar of a ball mill machine (Across International PQ-N2 Planetary, Livingston, New Jersey, USA). Five alumina ceramic grinding balls were also placed in each jar. The milling time varied from 8 h, 16 h, to 32 h. Light yellow fine powder was obtained after ball milling (Fig. 1b). Two control tests were also conducted by mixing powders milled at different time periods. The first one consisted of 8 h milled powder and 32 h milled powder at a 1:1 weight ratio. The second one consisted of 8 h, 16 h, and 32 h milled powder at a 1:1:1 weight ratio. The mixtures were placed in the ball milling jar without adding the ceramic ball and were mixed for 5 h.

#### 2.3 Thermomechanical and compositional characterizations

Dynamic mechanical analysis (DMA) of the as-prepared epoxy was conducted in multi-frequency-strain mode using a Q800 dynamic mechanical analyzer (TA Instruments, DE, USA). The amplitude was 20 µm, the frequency was 1 Hz, and the temperature sweep range was -30 to 200 °C. The temperature ramp rate was 3 °C min<sup>-1</sup>. A differential scanning calorimeter (DSC) study was conducted using a PerkinElmer DSC 4000 instrument (MA, USA). A small piece of as-prepared epoxy of approximately 7 mg was placed in an aluminum pan and scanned between -30 °C and 200 °C with heating and cooling rates of 10 °C min<sup>-1</sup>. The purging rate of the nitrogen gas was 30 mL min<sup>-1</sup>. Two cooling and heating cycles were conducted, and the second cycle is shown so that the thermal history is eliminated (see Fig. 2b). The glass transition temperature  $(T_{o})$  is labeled in the plot (see Fig. 2b). The as-prepared epoxy, selfhealed epoxies, and the powders at different healing or recycling cycles were characterized with a Nicolet 6700 FTIR spectrometer with a scan range of 4000-600 cm<sup>-1</sup>.

# 2.4 Compressive strength test

In order to investigate the compressive strength of the asprepared specimens, an isothermal uniaxial compression test was conducted using an MTS machine (Alliance RT/5, MTS, USA) equipped with a temperature-regulated oven fitted with a Eurotherm controller (Thermodynamic Engineering Inc., Camarillo, CA). Room temperature and 110 °C were selected, from glassy to rubbery temperatures, in order to fully understand the compression behavior of the recyclable epoxy. The loading rate was 1 mm min<sup>-1</sup> for all the specimens, and the data acquisition rate was 10 Hz. The control software used was Test Work 4. Four effective specimens were used for each test.

# 2.5 Self-healing experiments and healing efficiency calculation

Ball-milled epoxy powder was placed in a specially manufactured steel mold to perform the self-healing or recycling experiments. For the healing experiment, 1 g powder was consistently placed in the mold for all tests. The mold was placed in between eXpert 2610 MTS clamps (ADMET, Norwood, MA, USA). The control software was MTESTQuattro. The temperature in the thermal chamber was regulated by an E5AC-T digital controller (OMRON, Japan). Combinations of different temperatures (90, 115, 150, 180,

and 210 °C), compressive molding stress (3, 6, and 12 MPa), and healing time (1, 2.5, and 10 h) were tuned to investigate the influence of experimental conditions on the healing efficiencies of the recyclable epoxy. Pressure was applied to the mold at a rate of 500 N min<sup>-1</sup> (or 1.67 MPa min<sup>-1</sup>) until the designated values were reached. Then, the MTS clamp was held at the target position for a selected period of healing time. The slight pressure change due to reorganization of the molecules within the epoxy powder was tracked and is shown in the healing profile. The data acquisition rate during healing was 10 samples per min. All healed specimens had similar dimensions of 60 mm (length) × 5 mm (width)  $\times$  3 mm (thickness). The length and the width were determined by the dimension of the steel mold. The sample thickness was approximately 3 mm, which slightly varied due to the differences of temperature and pressure during the selfhealing experiments.

The healing efficiencies were determined by the uniaxial tension test. After healing, the healed specimens were subjected to the tensile test using an eXpert 2610 MTS (ADMET, Norwood, MA, USA). The tests were conducted at room temperature at a loading rate of 40 N min<sup>-1</sup> until fracture. The data acquisition rate was 120 points per min. The ratio of the average tensile strength of the healed specimen over the average tensile strength of the as-prepared specimen was defined as the healing efficiency. The healing test and the corresponding tensile test were repeated at least three times, and the average results and standard deviations are reported.

#### SEM visualization

The ball-milled powders at different healing cycles were visualized by scanning electron microscopy (SEM) (Quanta 3D FEG, Hillsboro, OR, USA) using secondary electrons. The sample surfaces were coated with platinum for approximately 6 nm. The accelerating voltage was 5 kV, and the working distance was 9-9.5 mm.

#### 3. Results and discussion

### Characterization of the recyclable epoxy

The as-prepared recyclable epoxy was first scanned by DMA for its thermomechanical property in the temperature range of -30 to

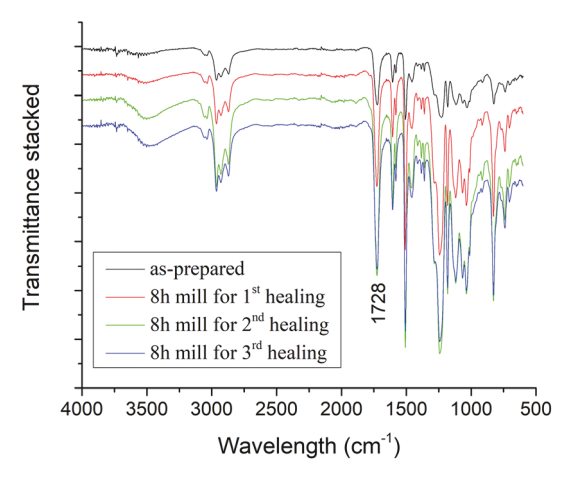
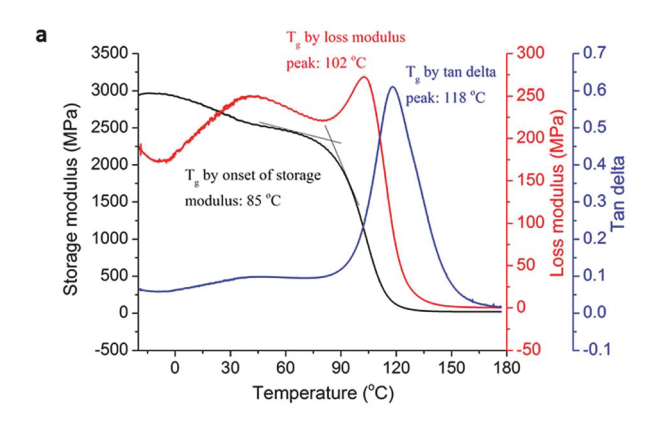


Fig. 3 FT-IR spectrum of the as-prepared epoxy and epoxy powders at different recycling cycles. The repetition of peaks suggests good recyclability.

200 °C (Fig. 2a). The glass transition temperatures  $(T_{\sigma})$  of the material are labeled on the basis of the onset of storage modulus, peak of loss modulus, and peak of tan delta. There are slight differences between the three  $T_{\rm g}$  values, which is common. The storage modulus of the epoxy is 2.7 GPa at 25 °C and it decreases to 118 MPa at 120 °C, which is stiffer than our previously developed epoxy with self-healing capability.43 DSC studies with two heating and cooling cycles were conducted between −30 to 200 °C (Fig. 2b). The second heating and cooling cycles are shown so that the thermal history of the material can be eliminated in the first cycle. The glass transition temperature  $(T_g)$  of the epoxy is 98 °C, as labeled in Fig. 2b.

The FT-IR spectra of the as-prepared epoxy and 8 h ballmilled specimens subjected to three healing cycles are displayed together in Fig. 3. The strong carbonyl stretch at 1728 cm<sup>-1</sup> indicates successful transesterification, which remains present in all samples, suggesting a reversible transesterification reaction. In addition, there is also no new peak formation and old peak disappearance, which indicate that the same functional groups are maintained in all samples during consecutive healing experiments.



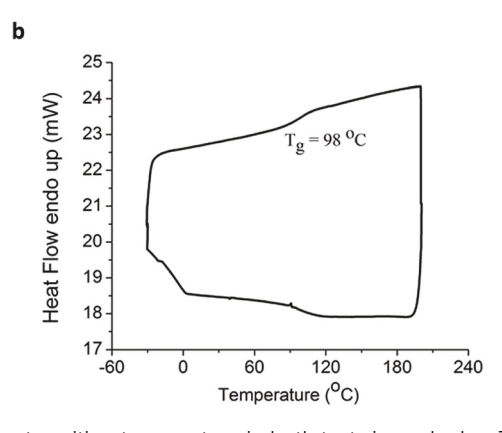


Fig. 2 (a) DMA temperature sweep and (b) second DSC heat flow scan. The glass transition temperature in both tests is marked as  $T_a$ 

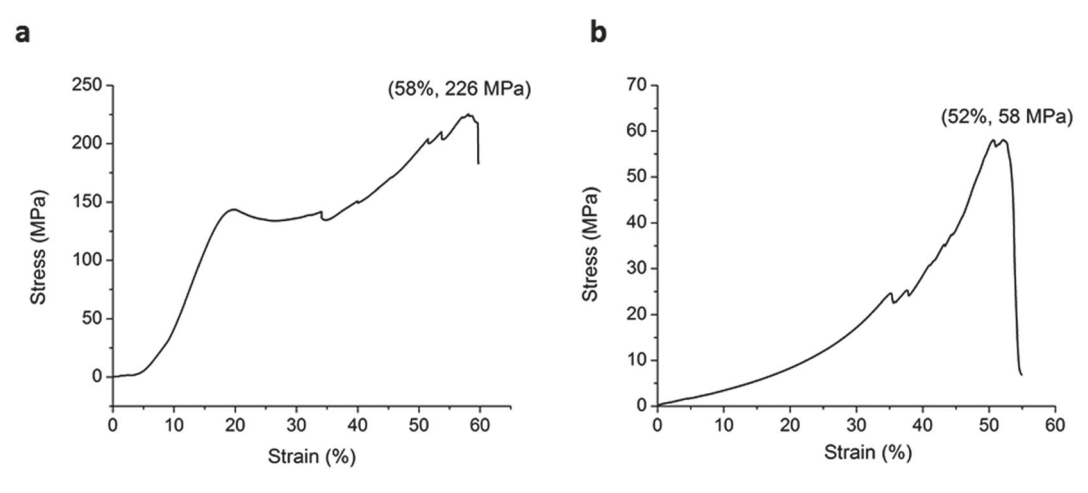


Fig. 4 Compressive strengths of the recyclable epoxy (a) at room temperature and (b) at 110 °C. The room temperature compression shows classical linear elastic, yielding, strain softening, plastic follow, and strain hardening behavior for typical glassy polymers. The high temperature test shows typical nonlinear rubber elasticity behavior. The cross-linked network leads to a rubbery epoxy that is also strong and stiff.

#### 3.2 Compressive strength

Compressive strength is an important parameter to evaluate in engineering materials that will be used for real-world applications. For this recyclable epoxy, a room temperature compression test was conducted first, as shown in Fig. 4a. The material experienced the yield point at 20% strain. When the compression strain reached 34%, a small crack was generated, and this contributed to a slight stress drop. Such small cracks also caused a similar stress drop later as compression continued. However, the sample did not break apart because it could still withstand the increasing load. At 58% strain, a relatively large crack was formed, and the compressive strength at this point was 226 MPa. The modulus calculated based on four compression tests at room temperature is 1.8 GPa. It is worthwhile to mention that this material did not break into pieces during the room temperature compression test. The loaded pressure only caused crack formation within the sample. The high toughness is an appealing feature for practical applications.

When compression testing the material at 110 °C, it behaved quite differently as compared to the compression test at room temperature (Fig. 4b). The first crack was formed at 35% strain, and the material was compressed into pieces at 52% strain with compressive strength of 58 MPa. As a comparison, the compressive strength was only 2.8 MPa to 5.0 MPa for our previously investigated self-healing epoxy system in the temperature range of 60-150 °C.43 It indicates that the curing agent is playing a crucial role in the mechanical properties of epoxy resins. The more rigid molecular structure of phthalic anhydride-cured recyclable epoxy demonstrated significantly improved mechanical properties as compared to the previous tricarballylic acid-cured system. Furthermore, the high compressive strength and stiffness at room temperature and the high glass transition temperature suggest that this new recyclable epoxy can be used in load-carrying structures.

#### 3.3 Self-healing and healing efficiency

The self-healing experiments were performed with a specially designed steel mold, as shown in Fig. 5a. The length of the

groove in the center of the mold is 60 mm and the width is 5 mm. The pressure bar in Fig. 5a perfectly fits the size of the groove. After carefully placing epoxy powders into the groove so that they are even with the surface, the pressure bar was placed on the top of the powders so that compressive force can be applied later through the bar. The same amount of epoxy powder (1 g) was placed in the groove for each specimen to keep the dimensions of the healed specimens consistent. The system was then put into the chamber of the MTS machine at a specific temperature for healing. The healing was conducted by compressing the pressure bar into the groove until a specific compressive stress was reached. After holding the compressive stress for the designed time period, the MTS machine was allowed to naturally cool to room temperature. The healed or recycled specimen was demolded, and it was then ready for the tensile test. Images of a self-healed specimen and a fractured one after the tensile test are shown in Fig. 5b.

Healing temperature, time, and pressure are well-known for their influences on healing efficiencies. In order to evaluate the effect of temperature on healing efficiency, five temperatures with one below  $T_{\rm g}$  (90 °C), one at approximately  $T_{\rm g}$  (115 °C), and three above  $T_g$  (150, 180, and 210 °C) were selected. Three sets of specimens were tested. In the first set of specimens (Groups 1-5), the healing time and pressure were kept at 2.5 h and 6 MPa,

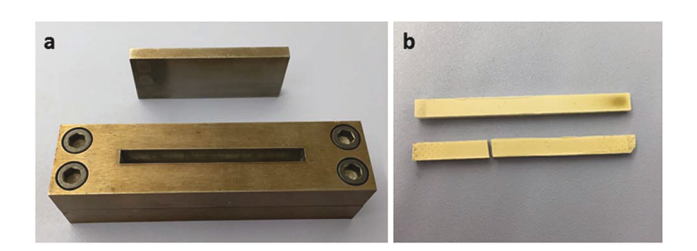


Fig. 5 Photographs of (a) the steel mold (bottom) and pressure bar (top) for preparing self-healing or recycling specimens, and (b) the healed epoxy specimen (top) and fractured specimen (bottom) after the tensile test.

Table 1 Effects of healing conditions on healing efficiency of the  $epoxy^a$ 

Group	Healing temperature (°C)	Healing time (h)	Healing pressure (MPa)	Tensile strength (MPa)	Healing efficiency (%)
1	90	2.5	6	$4.7 \pm 0.47$	11.4
2	115	2.5	6	$12.0 \pm 2.11$	29.1
3	150	2.5	6	$18.9 \pm 2.85$	45.9
4	180	2.5	6	$23.7 \pm 3.60$	57.5
5	210	2.5	6	$\textbf{31.0} \pm \textbf{2.94}$	75.2
6	150	1.0	6	$\textbf{11.0} \pm \textbf{0.01}$	26.7
3	150	2.5	6	$\textbf{18.9} \pm \textbf{2.85}$	45.9
7	150	10	6	$\textbf{31.7} \pm \textbf{2.62}$	76.9
8	150	2.5	3	$13.0\pm0.81$	31.6
3	150	2.5	6	$\textbf{18.9} \pm \textbf{2.85}$	45.9
9	150	2.5	12	$24.0\pm2.82$	58.3

<sup>&</sup>lt;sup>a</sup> Note: the tensile strength of the as-prepared epoxy is 41.2  $\pm$  6.08 MPa.

respectively. In the second set of specimens (Groups 3, 6, and 7), the healing temperature at 150  $^{\circ}$ C and the pressure at 6 MPa were maintained. In the third set of specimens (Groups 3, 8, and 9), the healing temperature of 150  $^{\circ}$ C and healing time of 2.5 h were maintained. For the first set of specimens, the healing profiles are shown in Fig. S2a,† and the tensile tests are shown in Fig. S2b in the ESI.† For the second set of specimens, the healing profiles are shown in Fig. S3a,† and the tensile tests are shown in Fig. S3b in the ESI.†

The tensile strength of the as-prepared epoxy with dimension 60 mm (length)  $\times$  5 mm (width)  $\times$  3 mm (thickness) is 41.2  $\pm$  6.08 MPa. This value will be used to calculate the healing efficiencies of all recycled samples.

The healing (recycling) condition, tensile strength values (average values of three tests), and calculated healing efficiencies for the three sets of specimens are listed in Table 1. The following observations can be made. (1) The healing efficiency increases with healing temperature. This trend is within our expectations because: (a) the transesterification reaction is more rapid at higher temperatures, and therefore, more ester

bonds form in between powder particles; (b) the modulus of the material decreases with the increase in temperature until 137 °C (stabilized after 137 °C), and therefore, the distance between particles becomes smaller with rising temperature and thus promotes the transesterification reaction. At 210 °C, the healing efficiency can reach 75.2%, which is fairly good. (2) It is clear that the tensile strengths exhibit an increasing trend with the increase in healing time. When translating the tensile strength to healing efficiency, a clear increase from 26.7% to 76.9% was noted when increasing the healing time from 1 h to 10 h. This is straightforward, as a longer healing time allows additional bonds to form via transesterification reaction. (3) Tuning the healing pressure exerts an effect that is similar to tuning the healing temperature and time, as expected. The healing pressure was selected to be at 3.0 MPa, 6.0 Mpa, and 12.0 MPa. The typical compressive load change with time during recycling and tensile stress-strain curves of recycled specimens are shown in Fig. 6a and b, respectively. The tensile strength of the healed specimen increased from 13.0 MPa to 24.0 MPa when the molding pressure was increased from 3.0 MPa to 12.0 MPa. The increased pressure can decrease the distance between particles, which ultimately will increase the surface contact and the transesterification reaction rate. (4) By elevating the temperature (for example, Group 5 versus Group 1) and/or increasing pressure (for example, Group 9 versus Group 8), the healing rate will be increased, i.e., a higher healing efficiency will be achieved within the same time period.

For the above experiments, the epoxy powders were obtained by ball milling for 8 h. In comparison, powders with a longer milling time and powder mixtures with different milling time periods were also studied, as shown in Fig. S4 in the ESI† and in Table 2, respectively. It can be seen that the healing efficiency was increased from 45.9% to 62.4% by simply changing the milling time according to Groups 3 and Group 10 in Table 2. This increase occurred because a longer milling time leads to smaller sized powders, thereby creating larger surface areas and more active sites for the transesterification reaction. However, a larger surface area associated with smaller particle size may need a longer reaction time to heal. Thus, long milling time is

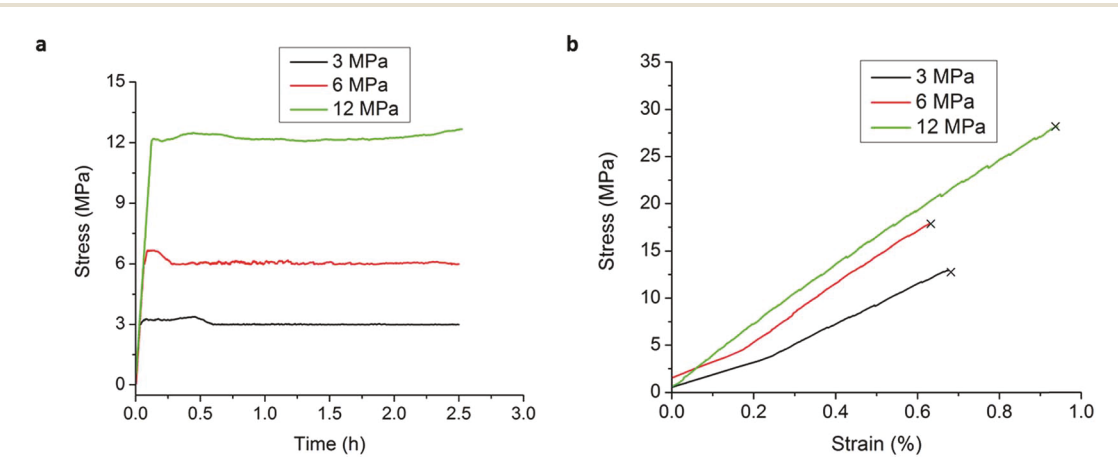


Fig. 6 Examples of (a) compressive load change with time during the healing process and (b) tension test results of healed specimens prepared at three different healing pressures (3 MPa, 6 MPa, and 12 MPa).

Group	Milling time (h)	Healing temperature (°C)	Healing time (h)	Healing pressure (MPa)	Tensile strength (MPa)	Healing efficiency (%)
3	8	150	2.5	6	$18.9 \pm 2.85$	45.9
10	32	150	2.5	6	$25.7\pm1.53$	62.4
11	32	150	10	12	$36.3 \pm 4.69$	88.1
14	8 h + 32 h (50.0 wt% each)	150	2.5	6	$26.7\pm2.52$	64.8
15	8 h + 16 h + 32 h (33.3 wt% each)	150	2.5	6	$23.3\pm3.51$	56.6

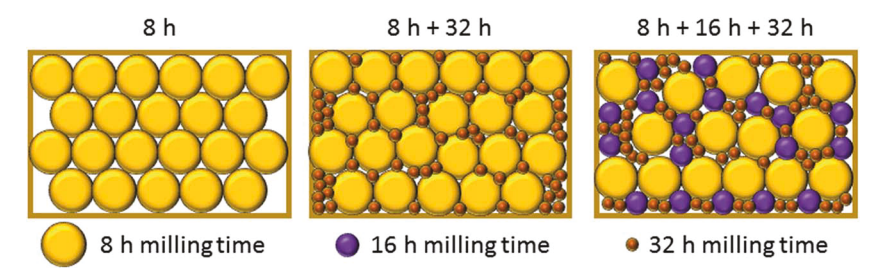


Fig. 7 Schematic of particle packing in powder mixtures prepared with powders of different sizes.

coupled with prolonged healing time and elevated healing pressure (Group 11, Table 2), and the highest healing efficiency achieved was 88.1%.

In order to increase the packing density of the powders so that more surface contact can be produced, we mixed powders milled for 8 h and 32 h at a 1:1 weight ratio by placing the mixture in the jar of the ball mill and mixing for 5 h without adding ceramic balls so that the particle sizes did not change. The results from Group 14 are comparable to that of Group 10 but much higher than that of Group 3, which indicates that adding epoxy powders with a smaller particle size will enhance the healing efficiency. A similar experiment was also conducted in Group 15 by mixing three types of powders with different milling times. Similar results were obtained, and the healing efficiency was clearly greater than that of Group 3.

Our explanation regarding epoxy powder mixing is illustrated in Fig. 7. With increasing ball milling time, the particle sizes of the recyclable epoxy became smaller, as illustrated by the gold, purple, and brown balls in Fig. 7. For specimens only containing 8 h milled powder, a large void space between particles decreased the surface contact area for the transesterification reaction and thus lowered the healing efficiency. Upon introducing much smaller particles milled for 32 h, the void space was partially filled, which led to a clear increase in the healing efficiency due to

an increased transesterification reaction in the particle contact area. For the three-component mixture, the result is not as efficient as the two-component system, and this may be attributed to less efficient particle packing of the three-component mixture as compared to the two-component mixture, which has denser packing. As will be seen later in the SEM observations, the powders are irregularly shaped instead of being perfectly spherical. Therefore, the classical packing theory based on spheres cannot fully guide the design of the mixture. Some empirical equations employed in determining densely graded aggregates in concrete design, which have particles with sharp angularities, may be referenced.<sup>45</sup>

Further cross comparison of the healing efficiencies from a different set of experiments gives us more valuable information regarding the recycling of this epoxy thermoset system. A comparison of Group 4 to Group 9 in Table 1 indicates that an increase of 30 °C on healing temperature has an effect similar to doubling the healing pressure; a comparison of Group 2 to Group 6 in Table 1 indicates that an increase of 35 °C has an effect similar to 2.5 times longer healing time; a comparison of Group 4 in Table 1 to Group 15 in Table 2 indicates that an increase of 30 °C has an effect similar to that of three-component mixing.

In addition to studying the healing efficiency of powders milled from as-prepared epoxy, we also investigated the

Table 3 Change of healing efficiency with healing cycles

Group	Healing cycle (h)	Healing temperature (°C)	Healing time (h)	Healing pressure (MPa)	Tensile strength (MPa)	Healing efficiency (%)
3	1 <sup>st</sup>	150	2.5	6	$18.9 \pm 2.85$	45.9
12	$2^{\mathrm{nd}}$	150	2.5	6	$35.6 \pm 4.51$	86.4
13	$3^{\rm rd}$	150	2.5	6	$23.7 \pm 6.02$	57 <b>.</b> 5

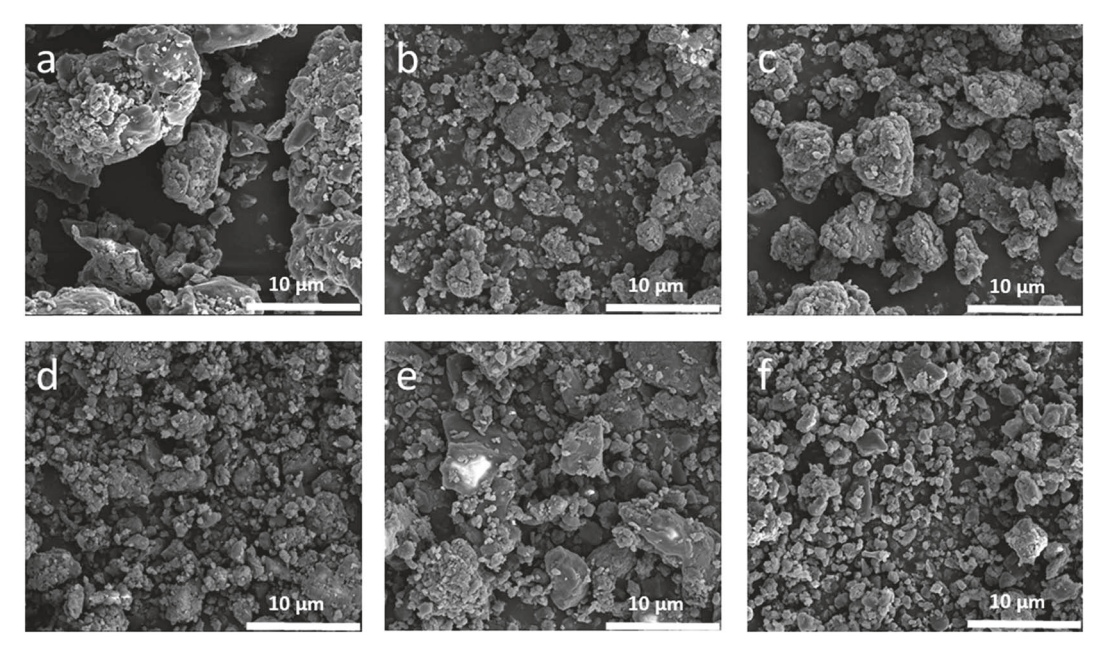


Fig. 8 SEM images of the recyclable epoxy powder at different healing cycles. (a) 8 h milled sample for the 1st healing experiment. (b) 8 h milled sample for the 2<sup>nd</sup> healing experiment. (c) 8 h milled sample for the 3<sup>rd</sup> healing experiment. (d) 32 h milled sample. (e) The mixture of 8 h and 32 h milled samples at a 1:1 weight ratio. (f) The mixture of 8 h, 16 h, and 32 h milled samples at a 1:1:1 weight ratio. All images are the same size for comparison.

repeatability of recycling. The healing process for milled powder from the as-prepared epoxy, epoxy after one, and two millinghealing cycles are denoted as the 1st, 2nd, and 3rd healing, respectively. The self-healing results are shown in Fig. S5 in the ESI† and also given in Table 3. The healing condition is the same for the three healing cycles at 150 °C healing temperature, 6 MPa healing pressure, and 2.5 h healing time. For the three

healing cycles, the healing efficiency is quite different, ranging from 45.9% to 86.4%, with the second healing cycle demonstrating the highest healing efficiency (Table 3). Based on previous experience, it is reasonable to believe that powder size difference and packing may play a role in this trend. Hence, we turned to SEM for a better understanding.

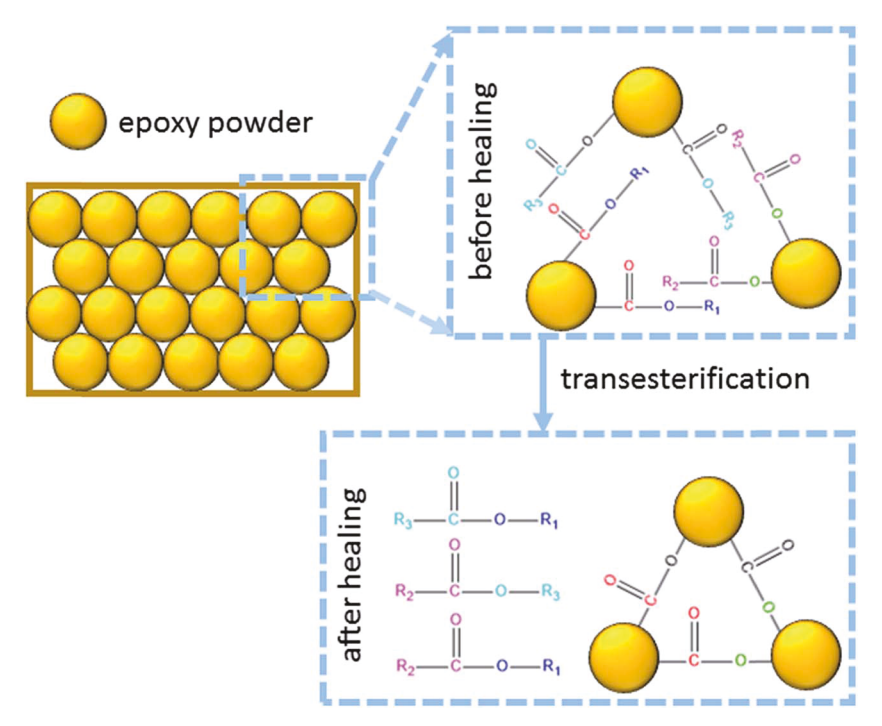


Fig. 9 Mechanism of the recycling of this thermoset epoxy system.

#### 3.4 SEM observations

In order to evaluate the impact of particle size on healing efficiency as mentioned above, SEM was employed to visualize the size and size distribution of ball-milled powder after consecutive milling-healing cycles, as shown in Fig. 8. For the 8 h milled specimen using the as-prepared epoxy (Fig. 8a), the particle size distributed in a certain range, with some big particles in the range of 10-20 µm and some small ones in the range of approximately 1 µm, which are attached to the bigger particles. The 8 h milled powder from the 1st healing sample is shown in Fig. 8b. The particle sizes become much smaller than that of Fig. 8a, in a range from approximately 0.1 μm to 8 μm. Surprisingly, the particle size, which is in the range of approximately 1  $\mu m$  to 9  $\mu m$ , for the milled 2<sup>nd</sup> healing sample (Fig. 8c) is smaller than that in Fig. 8a but larger than that in Fig. 8b. This explains the trend observed in Table 3, where the 2<sup>nd</sup> healing sample had the highest healing efficiency as compared to the 1st and 3rd healing samples.

For the 32 h milled powder (Fig. 8d), the particle size, with the majority in the range of approximately 0.1 μm to 5 μm, is much smaller as compared to Fig. 8a, ensuring a more closely packed system and enhanced healing efficiency. When mixing the 8 h (Fig. 8a) ball-milled powder with 32 h (Fig. 8d) ballmilled powder, both large and small particles can be seen (Fig. 8e). When compacted, the smaller sized particles may better fill in the open space within the skeleton formed by the larger sized particles, enhancing the particle-particle contact and self-healing efficiency. When mixing powders from 8 h, 16 h, and 32 h ball milling (Fig. 8f), there is a decrease in largesize particles because the content of 8 h milled powders decreased from 50% weight ratio to 33% ratio. However, when these more uniform particles are compacted, it may be difficult for them to form a dense configuration, leading to reduced healing efficiency as compared to that with 8 h ball-milled and 32 h ball-milled powder mixture.

#### 3.5 Mechanism

The powdered epoxy has a significant amount of ester bonds on the surface. If the environmental temperature is elevated and external pressure is applied to the epoxy powder, transesterification reactions occur and form new covalent bonds between particles at the interfaces, as shown in Fig. 9. A proposed mechanism showing the chemical details of the synthesis and self-healing process is included in the ESI in Fig. S6.† Byproducts will be generated, and these molecules will participate in a further transesterification reaction as long as high temperature and external load still exist. Once cooled to room temperature, the ester bonds will be in the "frozen" state rather than the "active" state that occurs under high temperatures. Therefore, no additional transesterification reaction will take place. Based on the explanation above, increasing temperature (that does not exceed the decomposition temperature, which is above 300 °C), and elevating pressure (that does not exceed the compressive strength at 58 MPa) will certainly increase the healing efficiency of the epoxy system. However, if the healing time is prolonged, the equilibrium state of the

transesterification reaction at the particle interface will eventually be reached so that the healing efficiency will become stable. Mixing particles with different sizes is also a good strategy to increase the healing efficiency because void space will be reduced in the system.

# 4. Conclusion

Successful synthesis of thermoset epoxy was accomplished using phthalic anhydride as the curing agent with a glass transition temperature at 98 °C based on the DSC test, room temperature modulus of 1.8 GPa, compression strength of 226 MPa at room temperature and 58 MPa at 110 °C, and tensile strength of 41.2 MPa at room temperature. The healing efficiency can be as high as 88.1%. It was shown that the solid recycling process is repeatable, suggesting that the epoxy can be used and reused several times. It was demonstrated that the recycling efficiency is affected by molding time, temperature, pressure, particle size, and particle size distribution. Within a certain range, higher healing temperature, increased healing pressure, and longer healing time almost always lead to higher healing efficiency. Smaller particle size obtained by prolonged milling time prompts a higher healing efficiency. A powder mixture with different milling times may also increase the packing density and the recycling efficiency. As compared to our previously developed tricarballylic acid-cured system, the reported epoxy system shows significantly improved mechanical properties with good recycling capability. This new recyclable epoxy has the potential to be used in load-carrying structures.

# Contribution

In this work, LL designed the synthetic strategy, prepared the recyclable epoxy, and conducted thermomechanical (DMA, DSC, compressive), SEM, and FTIR characterizations. JP conducted the ball milling, recycling, and tensile tests. GL provided guidance to the entire study. LL prepared the draft and GL revised the manuscript.

# Conflicts of interest

There are no conflicts to declare.

# Acknowledgements

The authors gratefully acknowledge the financial support by the National Science Foundation under grant number CMMI 1333997 and HRD 1736136, and NASA cooperative agreement NNX16AQ93A under contract number NASA/LEQSF(2016-19)-Phase3-10. Jian Pan also acknowledges the China Scholarship Council (201606840036).

### References

1 D. H. Turkenburg and H. R. Fischer, *Polymer*, 2015, **79**, 187–194.

Electronic Supplementary Material (ESI) for Journal of Materials Chemistry A. This journal is © The Royal Society of Chemistry 2017

# Recyclable High Performance Epoxy Based on Transesterification Reaction

Lu Lu, <sup>1</sup> Jian Pan, <sup>1,2</sup> Guoqiang Li\*

Department of Mechanical & Industrial Engineering Louisiana State University Baton Rouge, LA 70803, USA

<sup>1:</sup> Co-first author.

<sup>2:</sup> Visiting Ph.D. Student from the School of Mechanical Engineering, Nanjing University of Science and Technology, Xiaolingwei 200, Nanjing 210094, China.

<sup>\*</sup> Corresponding author. E-mail: <a href="mailto:lguoqi1@lsu.edu">lguoqi1@lsu.edu</a>; Tel.: 001-225-578-5302.

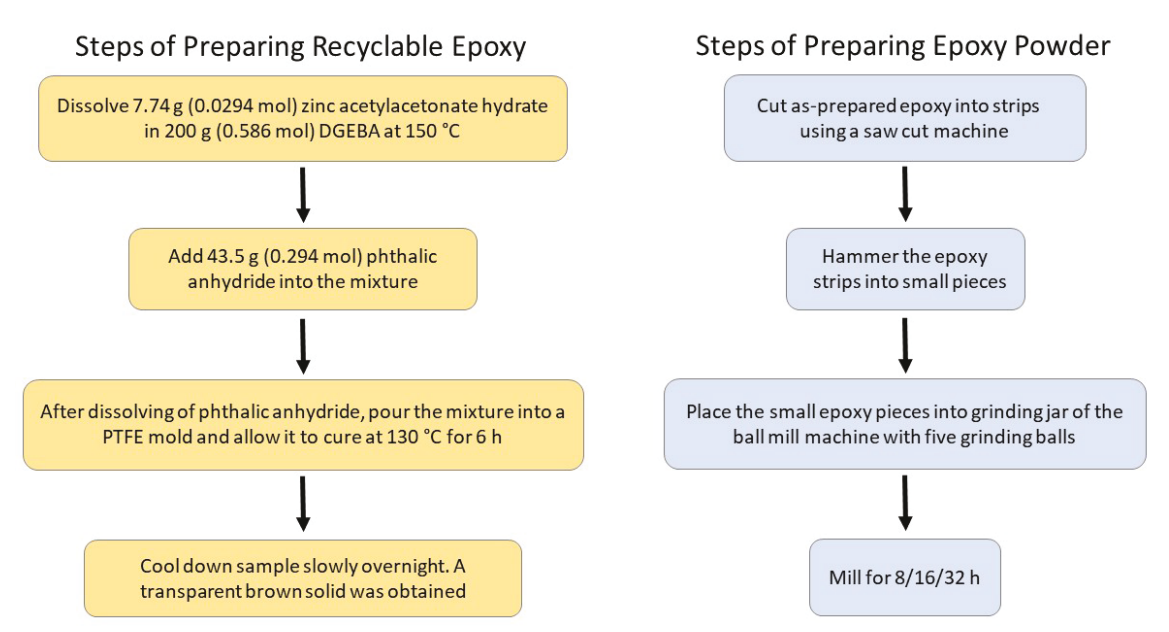


Figure S1. Flowchart of the recyclable epoxy and its powder form preparation process.

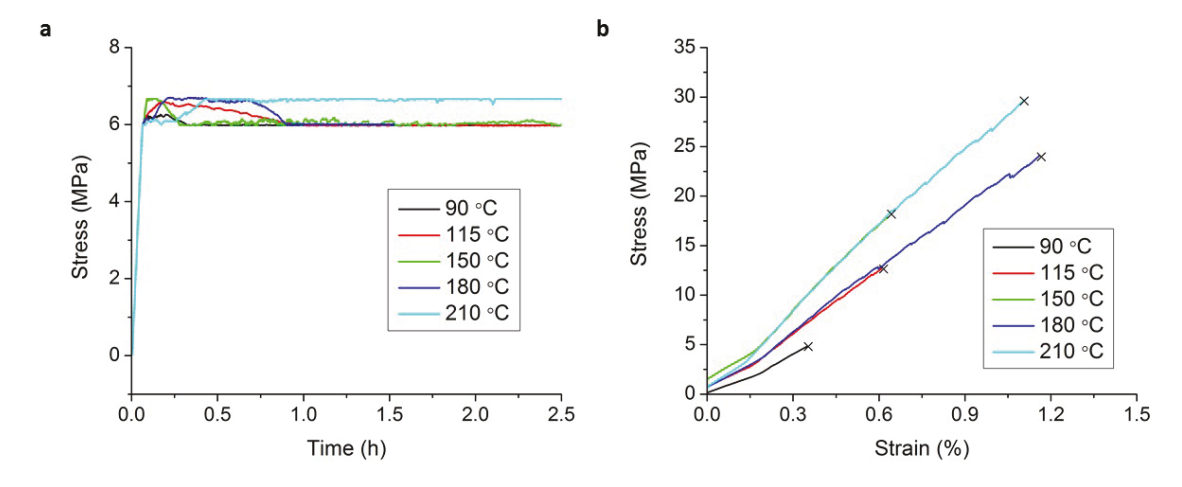


Figure S2. (a) Compressive load change with time during the healing process and (b) tensile stress-strain curves of healed specimens prepared at five different healing (recycling) temperatures.

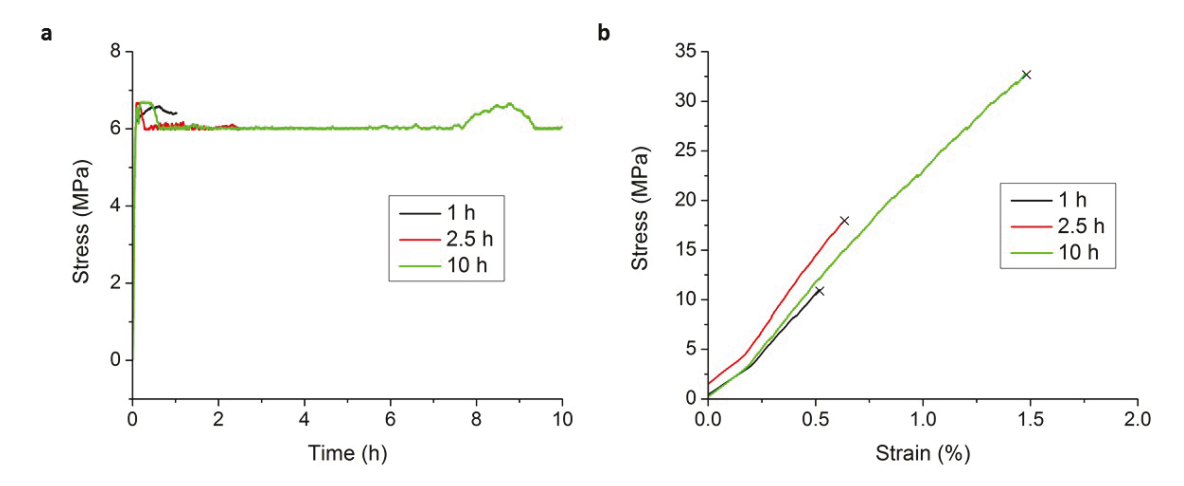


Figure S3. (a) Compressive load change with time during the healing process and (b) tensile stress-strain curves of healed specimens prepared at three different healing (recycling) durations.

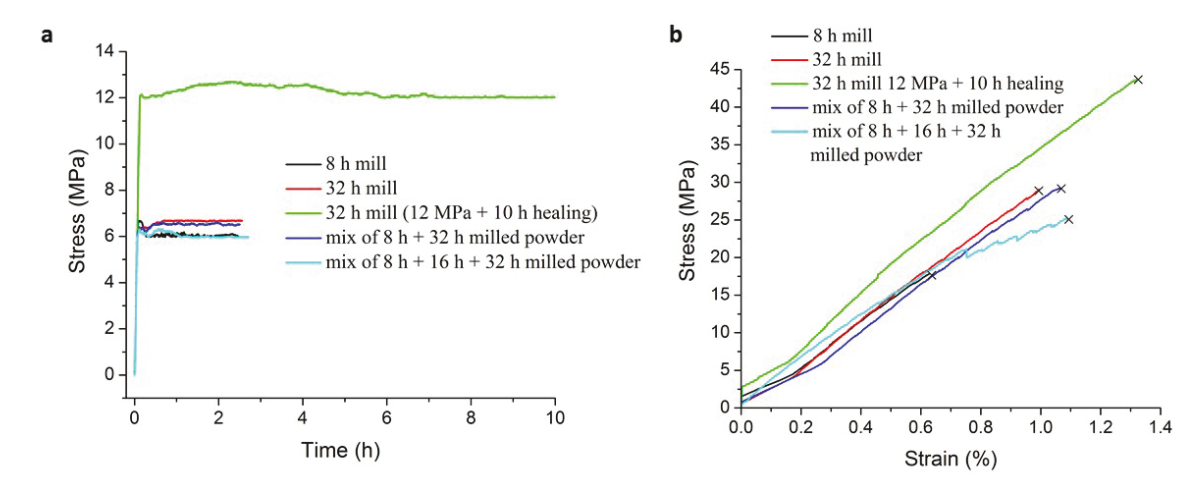


Figure S4. (a) Compressive load change with time during the healing process and (b) tensile stress-strain curves of healed specimens prepared with powders milled at different milling times or mixture of powders.

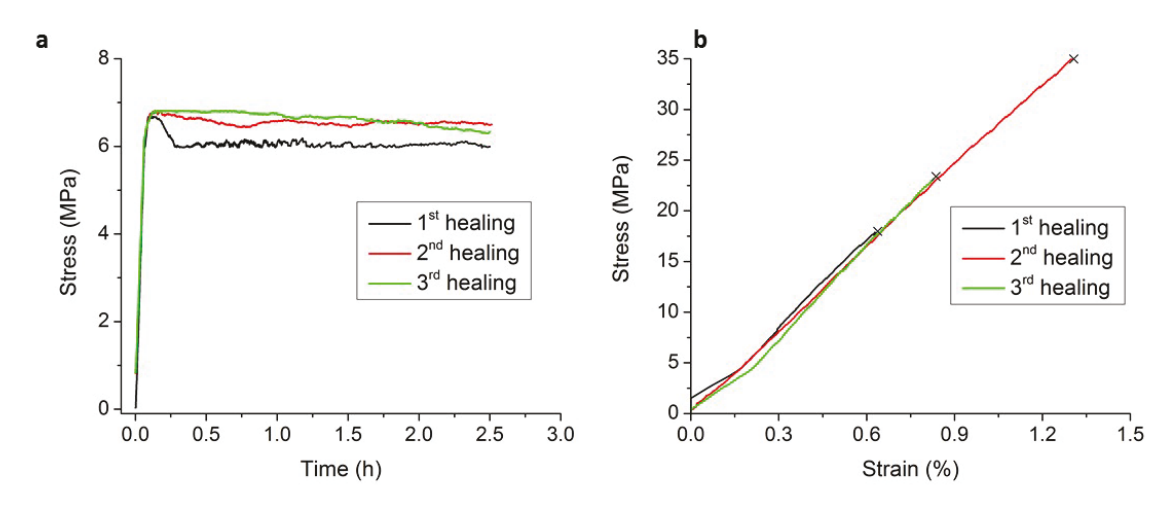


Figure S5. (a) Compressive load change with time during the healing process and (b) tensile stress-strain curves of healed specimens prepared after different healing (recycling) cycles.

Self-healing via transesterification

Figure S6. Chemical details of the synthesis and self-healing (recycling) process.

- 2 S. Kongparakul, S. Kornprasert, P. Suriya, D. Le, C. Samart, N. Chantarasiri, P. Prasassarakich and G. Guan, Prog. Org. Coat., 2017, 104, 173-179.
- 3 G. Li and V. D. Muthyala, Compos. Sci. Technol., 2008, 68,
- 4 G. Li and M. John, Compos. Sci. Technol., 2008, 68, 3337-3343.
- 5 S. R. White, N. R. Sottos, P. H. Geubelle, J. S. Moore, M. R. Kessler, S. R. Sriram, E. N. Brown and S. Viswanathan, Nature, 2001, 409, 794-797.
- 6 J. D. Rule, E. N. Brown, N. R. Sottos, S. R. White and J. S. Moore, Adv. Mater., 2005, 17, 205-208.
- 7 P. A. Pratama, M. Sharifi, A. M. Peterson and G. R. Palmese, ACS Appl. Mater. Interfaces, 2013, 5, 12425-12431.
- 8 E. N. Brown, S. R. White and N. R. Sottos, Compos. Sci. Technol., 2005, 65, 2474-2480.
- 9 T. Yin, M. Z. Rong, M. Q. Zhang and G. C. Yang, Compos. Sci. Technol., 2007, 67, 201-212.
- 10 Y. C. Yuan, M. Z. Rong, M. Q. Zhang, J. Chen, G. C. Yang and X. M. Li, Macromolecules, 2008, 41, 5197-5202.
- 11 Y. C. Yuan, X. J. Ye, M. Z. Rong, M. Q. Zhang, G. C. Yang and J. Q. Zhao, ACS Appl. Mater. Interfaces, 2011, 3, 4487-4495.
- 12 C. L. Mangun, A. C. Mader, N. R. Sottos and S. R. White, Polymer, 2010, 51, 4063-4068.
- 13 H. Jin, C. L. Mangun, D. S. Stradley, J. S. Moore, N. R. Sottos and S. R. White, *Polymer*, 2012, 53, 581-587.
- 14 R. Wang, H. Li, H. Hu, X. He and W. Liu, J. Appl. Polym. Sci., 2009, 113, 1501-1506.
- 15 D. S. Xiao, Y. C. Yuan, M. Z. Rong and M. Q. Zhang, Polymer, 2009, 50, 2967-2975.
- 16 E. L. Kirkby, V. J. Michaud, J. A. E. Månson, N. R. Sottos and S. R. White, Polymer, 2009, 50, 5533-5538.
- 17 T. S. Coope, U. F. J. Mayer, D. F. Wass, R. S. Trask and I. P. Bond, Adv. Funct. Mater., 2011, 21, 4624-4631.
- 18 X. Liu, H. Zhang, J. Wang, Z. Wang and S. Wang, Surf. Coat. Technol., 2012, 206, 4976-4980.
- 19 K. R. Hart, N. R. Sottos and S. R. White, Polymer, 2015, 67, 174-184.
- 20 M. Zako and N. Takano, J. Intell. Mater. Syst. Struct., 1999, 10, 836-841.
- 21 S. A. Hayes, F. R. Jones, K. Marshiya and W. Zhang, Composites, Part A, 2007, 38, 1116-1120.
- 22 J. Nji and G. Li, Polymer, 2010, 51, 6021-6029.
- 23 J. Nji and G. Li, Smart Mater. Struct., 2012, 21, 025011.

- 24 D. Montarnal, M. Capelot, F. Tournilhac and L. Leibler, Science, 2011, 334, 965-968.
- 25 M. Capelot, D. Montarnal, F. Tournilhac and L. Leibler, J. Am. Chem. Soc., 2012, 134, 7664-7667.
- 26 P. Taynton, H. Ni, C. Zhu, K. Yu, S. Loob, Y. Jin, H. J. Qi and W. Zhang, Adv. Mater., 2016, 28, 2904-2909.
- 27 Y. Meng, J. Jiang and M. Anthamatten, ACS Macro Lett., 2015, 4, 115-118.
- 28 X. Kuang, G. Liu, X. Dong, X. Liu, J. Xu and D. Wang, J. Polym. Sci., Part A: Polym. Chem., 2015, 53, 2094-2103.
- 29 T. S. Coope, D. H. Turkenburg, H. R. Fischer, R. Luterbacher, H. Van Bracht and I. P. Bond, Smart Mater. Struct., 2016, 25, 084010.
- 30 C. E. Yuan, M. Q. Zhang and M. Z. Rong, J. Mater. Chem. A, 2014, 2, 6558-6566.
- 31 Y. Z. Li, O. Rios, J. K. Keum, J. H. Chen and M. R. Kessler, ACS Appl. Mater. Interfaces, 2016, 8, 15750-15757.
- 32 H. Li, Y. Cui, H. Wang, Y. Zhu and B. Wang, Colloids Surf., A, 2017, 518, 181-187.
- 33 S. Khoee, S. H. Payandeh, P. Jafarzadeh and H. Asadi, Smart Mater. Struct., 2016, 25, 084014.
- 34 H. Yi, Y. H. Deng and C. Y. Wang, Compos. Sci. Technol., 2016, 133, 51-59.
- 35 P. Vijayan and M. A. AlMaadeed, eXPRESS Polym. Lett., 2016, 10, 506-524.
- 36 S. M. A. Hosseini, A. H. Jafari and E. Jamalizadeh, Electrochim. Acta, 2009, 54, 7207-7213.
- 37 P. Zhang and G. Li, Prog. Polym. Sci., 2016, 57, 32-63.
- 38 Y. Q. Wang, X. J. Cui, H. Ge, Y. X. Yang, Y. X. Wang, C. Zhang, J. J. Li, T. S. Deng, Z. F. Qin and X. L. Hou, ACS Sustainable Chem. Eng., 2015, 3, 3332-3337.
- 39 G. Oliveux, L. O. Dandy and G. A. Leeke, Prog. Mater. Sci., 2015, 72, 61-99.
- 40 Q. Shi, K. Yu, M. L. Dunn, T. Wang and H. J. Qi, Macromolecules, 2016, 49, 5527-5537.
- 41 K. Yu, P. Taynton, W. Zhang, M. L. Dunn and H. J. Qi, RSC Adv., 2014, 4, 10108-10117.
- 42 H. Yang, K. Yu, X. Mu, Y. Wei, Y. Guo and H. J. Qi, RSC Adv., 2016, 6, 22476-22487.
- 43 L. Lu, J. Fan and G. Li, Polymer, 2016, 105, 10-18.
- 44 W.-F. Su, Y.-C. Lee and W.-P. Pan, Thermochim. Acta, 2002, **392-393**, 395-398.
- 45 G. Li, Y. Zhao and S.-S. Pang, Cem. Concr. Res., 1999, 29, 839-845.